Correlation between Charge Transfer and Stick-Slip Friction at a Metal-Insulator Interface

R. Budakian and S. J. Putterman*

Physics Department, University of California, Los Angeles, California 90095

(Received 19 January 2000; revised manuscript received 11 April 2000)

Techniques have been developed that facilitate the measurement and imaging of the charge exchanged between metal-insulator surfaces in relative motion. In the regime where the forces of friction lead to stick-slip motion, we find that the charge transfer accompanying the slip events is proportional to the force jumps and is bunched at the stick locations. The constant of proportionality is measured in electron volts per angstrom and has a small variance over a large range of slip sizes, suggesting that in these experiments macroscopic friction originates from and scales to the intrinsic electronic interactions that form between metal and insulator surfaces.

PACS numbers: 46.55.+d, 73.20.Dx, 81.40.Pq

Friction and static electricity are everyday characteristics of surfaces in contact. Despite early phenomenological pictures by Coulomb and Da Vinci [1], a description of friction in terms of surface physics is still a matter of debate [2], and, despite its numerous applications [3], an understanding of contact electrification has "eluded researchers since the time of the ancient Greeks" [4,5].

It has been proposed [6] that a route to the explanation of friction lies in the discovery of the microscopic origins of stick-slip motion. Experiments using scanning probe microscopy have measured the interactions between a single asperity, the probe tip, and a variety of surfaces [7,8]. Although these experiments probe intrinsic electronic processes that contribute to friction, extrapolation to macroscopic systems and everyday friction is still being investigated [9]. Here, we study friction directly at the macroscopic level and, in addition to the force of friction, measure the charge transfer between metal and insulator surfaces in contact, which we find is quantitatively correlated with the force of friction. In our experiments, stick-slip friction is realized by sliding a 1 mm diameter gold ball on polymethylmethacrylate (PMMA). In the resulting stick-slip motion, each event is accompanied by a charge transfer that is quantitatively proportional to the size of the slip. We find that the unit for the ratio of the slip force to the number of charges transferred for a given event is an eV/Å, and furthermore this ratio remains constant over a large range of slip sizes and normal loads. We are thus motivated to use macroscopic measurements to propose a microscopic "bonding" model as the origin of friction for the systems studied. Electron volts and angstroms are the theoretically prescribed order of magnitude scale for bond energies and lengths (in fact, experiments which probe a single bond, e.g., gold to sulfur, suggest that the rupture force is about 1 nN [10]). These findings suggest that, for the systems reported in this paper, macroscopic friction can be quantitatively connected with the collective action of bonds that form at the interface between the metal and the insulator surfaces. While it is tempting to interpret these results in terms of individual bonds acting in parallel, the mechanism of their collective behavior is an open issue.

We picture the bonds as being formed by the difference in energy that exists between electrons in the donor states of the insulator and the metal work function [11–13]. Slipping occurs when the bonds snap and charge builds up as a result of electrons being stranded on the metal leaving the surface positively charged. The force of a single bond is remarkably large as an eV/Å is 1 nN so that

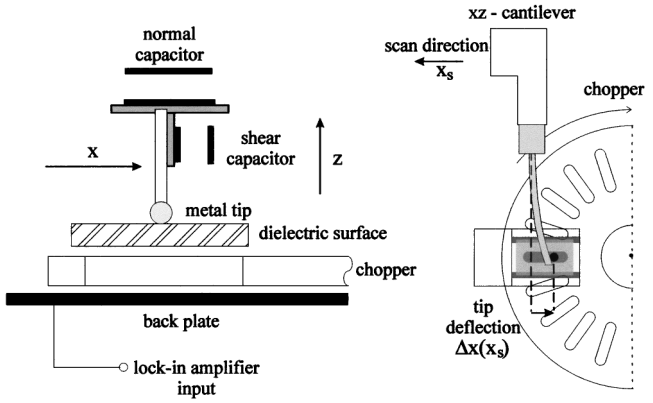

FIG. 1. Cantilever and integrated charge measurement apparatus: The xz cantilever is constructed by joining two pieces of spring steel joined perpendicular to one another, where the cross section of the joint forms a "T." The top piece is 3.6 mm wide, 4.3 mm long, and 330 μm thick, and is deflected vertically to apply normal force. The bottom piece is 3.2 mm wide, 1.6 cm long, and 100 μm thick, and bends laterally in response to a shear force. The tip used to scan the surface is made by attaching the metal sample, typically a 1 mm diameter gold ball or graphite rod, to the end of a glass capillary that is 2.5 mm long and 0.8 mm in diameter. By measuring the capacitance between a metal strip that is attached to each cantilever and a fixed plate, the deflection of each axis is accurately determined. The change in capacitance as a function of applied force (dC/dF) is then calibrated using a microbalance. For the results presented here, the dynamic response of the cantilever is measured with a time constant of 30 ms. Lateral displacement of the probe is preformed by rotating a micrometer screw which is attached to one axis of the translation stage. The screw is rotated using a stepper motor acting through a 100:1 gear head producing a displacement resolution of 30 nm. The net charge on the surface as a function of time or distance scanned is measured using a lock-in amplifier referenced to the 2 kHz chopper frequency.

 0031-9007/00/85(5)/1000(4)$15.00

10^8 bonds/mm^2, which is typical of our findings, corresponds to a force of 1 mN. This corresponds to an average macroscopic stress of about an atmosphere, and a focused stress at each bond of a Mbar ($\approx$1 eV/Å^3).

The experimental apparatus consists of a metal tip mounted on the end of an xz cantilever, shown in Fig. 1. It is scanned over a dielectric surface with a three-axis translation stage. The vertical (z) displacement of the cantilever is used to apply a normal force, while the lateral (x) deflection measures the frictional force. These deflections are measured independently using an ac capacitance bridge. In order to measure the integrated charge on the surface, a grounded metal chopper is placed between the back of the dielectric sample and a metal plate. The rotating slots on the chopper produce a time varying current on the metal plate where the amplitude of the induced current I_0 is proportional to the integrated charge on the surface $\gamma eN(x_s) = I_0/\omega_c$; e is the electron charge, ω_c is the angular frequency of the chopper, and γ is a geometric scaling factor due to the chopper which accounts for the fraction of charge induced on the back plate. The scanned distance x_s is the relative motion between the tip and the surface in the absence of friction. The value of γ is determined numerically by solving for the electric field on the back plate from a point charge on the dielectric surface. Thus, we are able to correlate the accumulated charge $N(x_s)$ with the friction force $F_s(x_s)$. A polymer dispersed liquid crystal (PDLC) layer placed just below the dielectric is used to image the charge distribution. Transmission of light through the PDLC is a function of electric field which depends on the local charge density [14]. Previous experiments between metals and polymer surfaces suggest that charge transfer is insensitive to the details of sample preparation such as surface defects and chemical impurities [11]. We find that in order to obtain reproducible results surface preparation and ambient conditions need to be reasonably controlled. After a general cleaning procedure, the sample is rinsed in a bath of high purity acetone, with the exception of PMMA; it is then washed in ethanol to remove residual acetone and finally rinsed under flowing 18 MΩ cm deionized water to remove the residual ethanol. The sample is then placed into a 50 mTorr vacuum where it is dried using a 20 W halogen bulb. Data for PMMA and quartz are obtained under vacuum since both the charge and friction measurements are sensitive to outside humidity.

Figure 2 displays the density of charge left on a nylon surface after being scanned by a graphite tip under ambient conditions. Also displayed is the time averaged stick-slip motion where the regions of sticking appear white. One notes that charges are bunched at just those locations where stick events are observed and that typical charge densities are 10^8 charges/mm^2. Figure 3(A) shows the force of friction as a function of distance scanned as well as the total charge laid down on the surface for a gold tip in contact with PMMA. Note that each slip event in Fig. 3 reveals a jump in the accumulated charge, and furthermore there exists a scale factor 0.48 $\pm$ 0.02 eV/Å which can be used to collapse these two measurements onto one curve as shown in Fig. 3(B).

To calculate the scaled curves, we introduce the displacement Δx_i of the tip on the ith slip event which is resisted by a force, $\Delta F_i = k\Delta x_i$, where k is the lateral spring constant of the cantilever. The total distance x_s

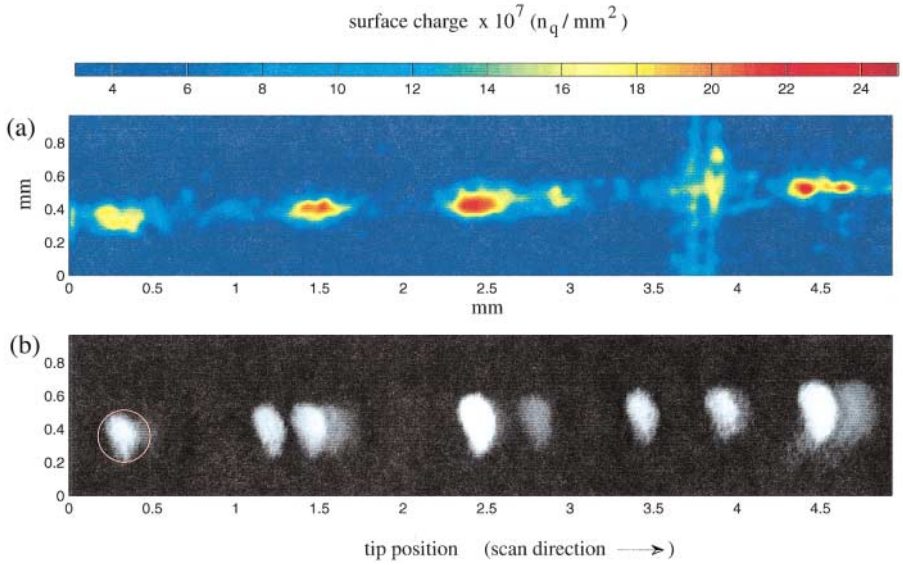

FIG. 2 (color). (A) Electrification and stick-slip motion, showing the distribution of positive charges that are left behind after a polyester surface is scanned by a 0.3 mm diameter graphite tip that is attached to the xz cantilever shown in Fig. 1 (below). The surface is scanned under ambient conditions with 2 mN normal force applied to the tip at a scan velocity of 170 μm/s. The residual surface charge is imaged in 333 ms using the liquid crystal apparatus. The charge image is taken after the surface has been scanned and the tip is retracted. (B) Tip motion during scan: The image shows the time averaged position of the tip recorded during the scan at 30 frames per second. The physical dimension of the tip is indicated by the circle. Brighter regions indicate longer stick times.

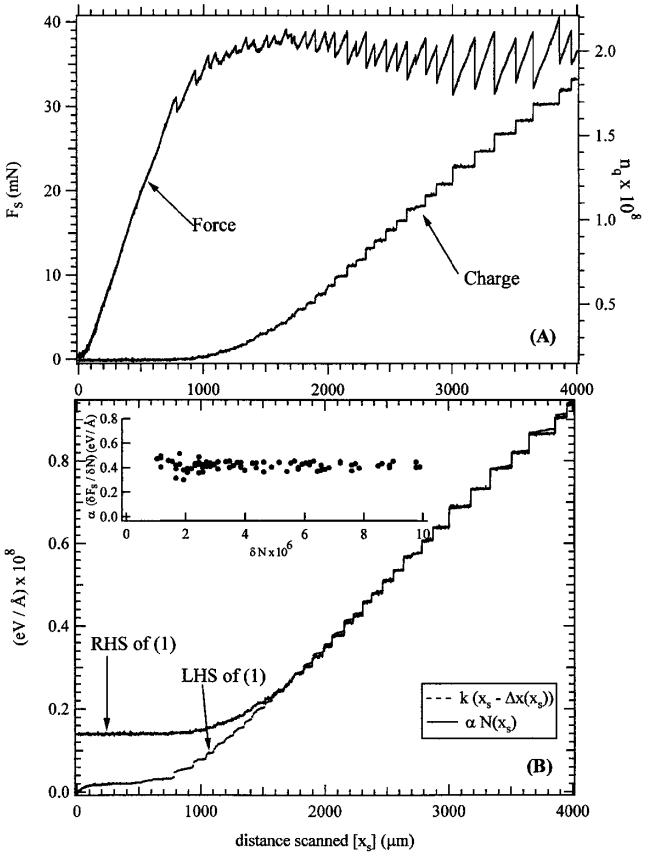

FIG. 3. (A) Correlation between deposited charge and friction force: Simultaneous measurement of friction force and surface charge from a scan of a 1 mm diameter 99.99% purity gold ball tip on a smooth PMMA surface. The PMMA sample is obtained by cutting a 1 cm × 1 cm piece of a 1.3 mm thick compact disk after the protective coating on the disk is carefully removed. The scan is preformed by applying a 95 mN normal force and scanning at 10 μm/s. Initially, the tip is stuck to the surface and the shear force builds up to an average value of 35 mN before the stick-slip instability starts. The integrated charge on the surface is zero during the time the tip is stuck and increases in steps corresponding to the slips between the tip and the surface. The amount of charge deposited is indicated on the right-hand axis in units of 10^8 charges, where the sign of the charge is positive. (B) Scaled force and charge curves: The dotted curve represents the left-hand side of Eq. (1) calculated using the cantilever deflection $\Delta x(x_s)$ shown in (A) and the spring constant $k = 47$ N/m. The value of α used for the right-hand side of Eq. (1) is determined from the slope of this curve in the limit $x_s \gg \Delta x$. For measurements made where the normal force is varied between 68 and 106 mN, $\alpha = 0.48$ eV/Å. The inset shows the value of α as determined from the individual slip events in the same range of normal force. Note that α remained the same over a range of slip events whose magnitude varied by a factor of 10. Charge has been offset for (B). This offset can be interpreted in terms of the screened charge under the tip and the elastic springback [27] of the tip.

scanned by the stage obeys

$$x_s = \sum_{i<s} \Delta x_i + \Delta x(x_s),$$

where $\Delta x(x_s)$ is the deflection of the tip from its position of mechanical equilibrium after being scanned a distance x_s. Setting $\Delta F_i = \alpha \Delta N_i$ and summing over all events yields

$$k[x_s - \Delta x(x_s)] = \alpha N(x_s), \quad (1)$$

where ΔN_i is the charge transferred on the ith event, $N(x_s)$ is the total charge deposited in scanning x_s, and α is the average lateral force per charge. The force curve in Fig. 3(A), which is equal to $k\Delta x(x_s)$, has been combined with the imposed x_s to obtain a scaled force curve equal to the left-hand side of Eq. (1). This is plotted in Fig. 3(B) along with $\alpha N(x_s)$, using the value 0.48 eV/Å for α. (Note that the energy U_b stored in the bonds is small compared to the energy stored in the cantilever U_s. Prior to the slip $U_b/U_s \approx k/k_b \Delta N_i \ll 1$, where the spring constant of a bond $k_b \approx 1$ eV/Å^2.)

The energy and length scales that combine to determine α are characteristic of a single molecular bond, which suggests that in these experiments friction arises from bunches of bonds that form between and grab to rest two surfaces in relative motion. (By ascribing the measured friction forces to the bonds, we have neglected the collective Coulomb electric forces that exist between the dielectric and their image in the tip.) The charge transfer is a marker for the number of bonds ruptured at a particular slip event. Our claim that the charges are bunched is key to our interpretation of the data. In addition to Fig. 2, evidence for the bunching of charge is provided by the following: (i) contact spectroscopy measurements on PMMA and a group of metals which indicate that charge transfer occurs approximately within a 0.4 eV window between the surface states of PMMA and the metallic Fermi level [12], consistent with the value of α determined above; (ii) the value of α and therefore the integrated charge transferred in a scan of length x_s is independent of the normal force [see inset of Fig. 3(B)] as required by Eq. (1) which yields for the limiting rate of charge transfer $dN/dx = k/\alpha$—while the average size of an individual sticking event increases with the load, there are fewer but larger events for the given distance traveled; (iii) measurements of charges transferred by lowering and retracting the tip to one spot on the surface. Here, the deposited charge is proportional to the normal force, which is consistent with other measurements that show the real area of contact increases with the applied load [15,16]. Had charges in our experiment been deposited uniformly with distance scanned, then one would expect dN/dx to increase with normal force, which as we said is not the case.

Equation (1) is in a form that also fits the data for sliding friction as shown in Fig. 4, where the force of friction between gold and quartz is measured. Even in the absence of stick-slip events, one finds that variations in F are accompanied with proportional variations in N with a similar value of α measured in eV/Å. In order to determine the applicability of this model to sliding friction, future experiments need to be performed which study the transition from stick-slip to sliding friction by varying the spring constant of the cantilever and the normal force.

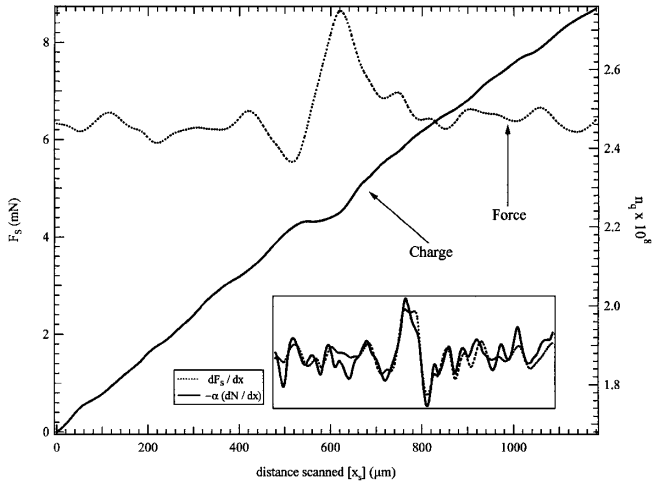

FIG. 4. Force and charge data for sliding friction: Scan of 1 mm diameter gold tip on the surface of a 1 cm $\times$ 1 cm, 3 mm thick optically flat piece of fused quartz. The surface is scanned with 150 mN normal force applied to the tip at a scan velocity of 5 μm/s. The value of α for the interface of gold and quartz is determined through Eq. (1) to be 0.31 eV/Å. This value for α also matches the fluctuations in the shear force and the deposited charge as shown in the inset.

Our interpretation of friction in these systems as being due to the formation of bonds that grab to rest the sliding surfaces and then rupture as the stress builds up has a number of consequences. When the probe is stuck, forces which stretch the bonds should encounter a resonant response determined by a frequency $\omega \approx [N_i k_m/m]^{1/2}$, where k_m is the spring constant of an individual molecular bond and m is the mass of the tip. Approximating k_m by α/Å leads to resonance in the MHz range for a 1 mg mass. We note that in this picture of friction the bonding between surfaces should not be viewed as a solid material bridge, but rather as a network of bonds whose density we presume displays structure on many length scales. Such networks can be expected to exist inside of real materials so that fatigue and hysteresis could have contributions from bond rupture as well as the growth of Griffith cracks [17] and their Barenblatt [18] generalizations. Rupture of bonds, whether on the surface or in the bulk, should be accompanied by an acoustic emission also known as the Kaiser effect [19,20], and as found by Pasztor and Schmidt training can be observed as stresses are cycled and bond clumps not rigid enough to withstand that stress value are swept out. The time scales for charge transfers connected with sliding surfaces can be under 200 ps [21]. Although such observations motivated the present investigation, we have not yet measured the time scale of the bond rupture events.

Other processes studied with the goal of elucidating the fundamental basis of friction include plastic deformation, bridging between surfaces and fracture at "cold welded" junctions [1,22], electron-phonon interactions between metals and atomic layers of adsorbed gasses [23], and liquid-solid phase transitions in lubricated layers [24]. An alternative interpretation of the role of electrostatic forces in friction is provided by Derjaguin's analysis of the surface double layer that forms at the interface of a dielectric and a metal [25,26].

Macroscopic measurements of metal-insulator surfaces in relative motion suggest that triboelectrification and friction have a common origin, namely, bond formation and rupture.

We acknowledge valuable discussions with L. Knopoff, P. Evans, M. Fisher, and also K. Holczer for valuable assistance in the experimental design. This research is supported by the U.S. Department of Energy (Division of Engineering Research).

*To whom correspondence should be addressed.

[1] F. P. Bowden and D. Tabor, *The Friction and Lubrication of Solids* (Clarendon Press, Oxford, 1986).
[2] J. Krim, Sci. Am. **275**, No. 4, 74 (1996).
[3] B. Maurer, Chem. Ing. Tech. **51**, 98 (1979); C. Holt, Sci. Am. **275**, No. 4, 128 (1996).
[4] B. D. Terris, J. E. Stern, D. Rugar, and H. J. Mamin, Phys. Rev. Lett. **63**, 2669 (1989).
[5] A. D. Moore, *Electrostatics* (Doubleday, New York, 1968).
[6] B. N. J. Persson, *Sliding Friction* (Springer-Verlag, Berlin, 1998).
[7] K. Feldman, T. Tervoort, P. Smith, and N. D. Spencer, Langmuir **14**, 372 (1998).
[8] G. Hähner and N. Spencer, Phys. Today **51**, No. 9, 22 (1998).
[9] A. R. C. Baljon and M. O. Robbins, Science **271**, 482 (1996).
[10] M. Grandbois, M. Beyer, M. Reif, H. C. Schaumann, and H. E. Gaub, Science **283**, 1727 (1999).
[11] A. R. Akande and J. Lowell, J. Phys. D **20**, 565 (1987).
[12] T. J. Fabish and C. B. Duke, J. Appl. Phys. **48**, 4256 (1977).
[13] L. H. Lee, J. Electrost. **32**, 1 (1994).
[14] R. Budakian and S. J. Putterman, Rev. Sci. Instrum. **71**, 444 (2000).
[15] J. H. Dieterich and B. D. Kilgore, Tectonophysics **256**, 219 (1995).
[16] B. A. Kwetkus, K. Sattler, and H. C. Siegmann, J. Phys. D **25**, 139 (1992).
[17] S. P. Timoshenko and J. N. Goodier, *Theory of Elasticity* (McGraw-Hill, New York, 1970).
[18] L. D. Landau and E. M. Lifshitz, *Theory of Elasticity* (Addison-Wesley, Reading, MA, 1970).
[19] G. Pasztor and C. Schmidt, J. Appl. Phys. **49**, 886 (1978).
[20] T. Erber, S. A. Guralnick, R. D. Desai, and W. Kook, J. Phys. D **30**, 2818 (1997).
[21] R. Budakian, K. Weninger, R. A. Hiller, and S. J. Putterman, Nature (London) **391**, 266 (1998).
[22] K. L. Johnson, *Contact Mechanics* (Cambridge University Press, Cambridge, England, 1985).
[23] C. Daly and J. Krim, Phys. Rev. Lett. **76**, 803 (1996).
[24] B. Bhushan, J. N. Israelachvili, and U. Landman, Nature (London) **374**, 607 (1995).
[25] B. V. Derjaguin and V. P. Smilga, Wear **7**, 270 (1964).
[26] P.-G. de Gennes, *Soft Interfaces* (Cambridge University Press, Cambridge, England, 1997).
[27] E. Rabinowicz, *Friction and Wear of Materials* (Wiley, New York, 1965).